Site-site interaction model for alcohol models in two-dimensions

Aurélien Perera

Site-site interaction model for alcohol models in two-dimensions

Aurélien Perera*

September 23, 2024

Laboratoire de Physique Théorique de la Matière Condensée (UMR CNRS 7600), Sorbonne Université, 4 Place Jussieu, F75252, Paris cedex 05, France.

Abstract

An interaction site-based model of two-dimensional alcohols is proposed as a follow up of the recent SSMB site-site model for 2D water [*J. Mol. Liq. 386 (2023 122475*]. Computer simulation studies indicate that the model exhibits hbond-type clustering based on the same charge order feature observed in real alcohols. Hence, the equivalent of 2D mono-ols ranging from methanol to octanol were studied for their clustering properties, focusing on how the micro-structure affects the shape of the site-site pair correlation functions and structure factors, as well as the combination of the latter into the radiation scattering intensities. The major finding is the apparent contradiction between the existence of large pre-peaks in the structure factors, usually associated to the existence of clusters, and the exponential decay of the cluster distribution indicating the absence of specific clusters, contrary to the 3D case. This is resolved by realizing that the pair correlation function is an observable of the local density fluctuations, hence the pre-peak witnesses fluctuations around clustering tendencies, which are the result of charge ordering of the polar groups, and visible in the snapshots. The scattering pre-peak witnesses only fluctuations due to charge ordering, and not the clusters themselves, underlining the fact that these are labile entities. The study highlights how charge order through atomic sites is a universal feature behind the micro-structure of organized liquids, and, in the particular case of 2D liquids, a more realistic alternative to orientation based models such as the Mercedes-Benz model, for instance.

1 Introduction

Since the introduction of two-dimensional Ising model,[1] our understanding of the relationship between the microscopic properties of matter and the macro-

*email: aurelien.perera@sorbonne-universite.fr

scopic properties have have been greatly improved, particularly in what concerns phase transitions.[2,3] For realistic liquids, two-dimensional models of hard discs[4] and Lennard-Jones liquids[5] have merely served as mimics of their three-dimension counter-parts, serving mostly to test simulations and theories. However, liquids can be classified into two categories; simple and complex liquids.[6] Liquid nitrogen is a canonical example of simple liquid that can be modeled by a Lennard-Jones atom.[7] These liquids have greatly helped improve our theoretical approach based on statistical mechanics, which was once considered as impossible by Lev Landau himself, as cited by P. G. de Gennes in.[8] But this is not the end of the story, when complex associating liquids such as water come into play. Indeed, water is an hydrogen bonding liquid[9] and this directional bonding gives water the status of special liquid, with more than 60 anomalous properties in the liquid phase alone. Because of this special interaction, water remains a liquid which is considered as not fully understood from microscopic point of view, both as a single component and more so when it is in mixing conditions.[10] In particular, our theoretical understanding from statistical physics point of view is still in infancy. A quick view of why this is so, can be obtained by modeling the hydrogen bonding property by a simple classical Coulomb charge association. This is possible by attributing a negative charge to the oxygen atom (usually around -0.7e) and a positive charge to the each of the two hydrogen atoms (usually around -0.3e). Coulomb charge association being about 557 times greater than the van de Waals interaction at distances above molecular contact, in dense liquid phase context, one has labile cluster formation which give water a two state dynamics, that of free and bound molecules. This two state model was formulated on a macroscopic basis by Röntgen and corresponds to one of the earlier models of water. In this context, unlike simple liquids, it is really useful to have a two-dimensional counterpart, in order to disentangle the various contributions between microscopic and macroscopic properties, which make water a liquid difficult to fully understand. The Mercedes-Benz (MB) model[11,12] have been a good example of such two-dimension model.

The MB model is purely orientational, similar to the dipole representation of water. We have recently introduced a 2D water model based on charged site representation, the SSMB model[13] , which mimics real water on the basis of atom-atom interaction. While very similar to the original MB model, it was found to produce a more realistic pair correlation function, similar to that of real water, and more importantly, a pair structure factor with the characteristic shoulder peak of the x-ray spectra of real water,[14,15] which is absent for the MB model. This is an important point because it witness the microscopic dual state of water, not in real space, as postulated by the MB model, but in the reciprocal space, as found for the real water. In addition, it should be noted that the pair correlation function plays a capital role in the statistical physics based description of disordered liquids, unlike ordered liquids (such as in the Ising model for instance), where it is the one body correlation function which correspond to the order parameter. This function describes better the local disorder, and is a capital indicator of the difference between simple and complex liquids.

Alcohols have played an important role in the comprehension of complex liquids, since these liquids tend to form local hydrogen bonded clusters which are visible from the x-ray scattering spectra, through the characteristic pre-peak in the range $k \approx 0.5 - 1\mathring{A}^{-1}$,[16] unlike water, for which such clusters exists, but do not produce a well separated pre-peak, but merely a shoulder peak.[15,17] This is very intriguing, since hydrogen bonding in water plays a more important role than it does for alcohols, even though both are associating liquids. For instance, alcohols are not know to possess the many anomalous properties that water does. In this context, it appears as necessary to have a site interaction 2D model of alcohols, as a complement to that of water. Indeed, an equivalent of the MB model for alcohols have been introduced previously[18] and a structural analysis of the model was presented recently by Urbic.[19]

The present work aims at extending the MB-like model of alcohols to a site-site representation, which would be an equivalent of the SSMB model to the MB water model. Since our calculations are in the Canonical Ensemble at constant NVT, as opposed to those of Ref.[19] in the isobaric ensemble with constant NPT, we impose the same packing fraction in order to compare different alcohols. In addition, we compute the site-site structure factors and the equivalent of the scattering intensity, which is one way to validate the models by comparing the pre-peaks and their dependence in alkyl tail length and temperature to that obtained from experiments[16] .

2 Model, theoretical and computational details

2.1 2D alcohol models

The interaction site based two dimensional alcohol models follow the same patterns we have previously developed in the case of 2D site-site SSMB model of water.[13] Namely, we replace the interaction between the MB arms by "charged" site interactions, combined with a repulsive interaction site. This is illustrated in Fig.1.

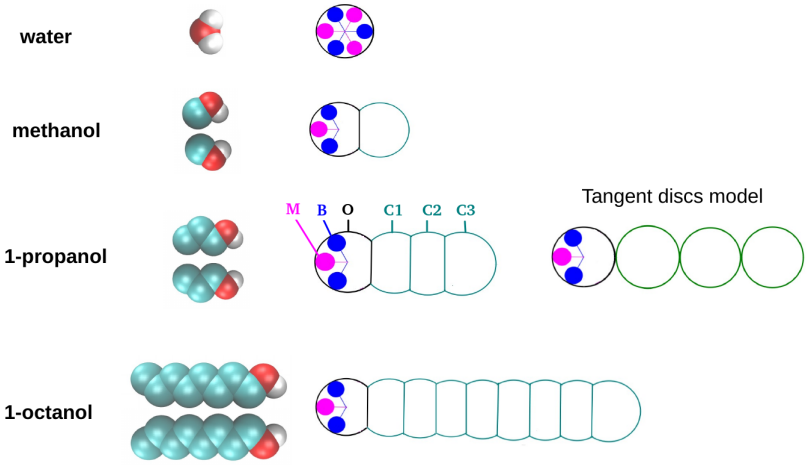

Figure 1: Illustration of the 2D non-chiral alcohol models, compared to their 3D/2D realistic chiral models (see text). The site-site equivalent of 2D 1-propanol model of tangent discs of Ref.[19] is shown for comparison. The site-site water model of Ref.[13] is equally shown for comparison. For the real molecules, oxygen site is red, hydrogen in white and methyl/methylene site in green. For the 2D acohols, the hydroxyl head is black circle, the attractive sites are in blue, repulsive in magenta, and methyl sites are green circles. The sites positions are explained in the text. The nomenclature for naming site is illustrated for the propanol molecule.

The hydroxyl head group is modeled as a 2 arms state, with 2 attractive sites (in blue in Fig.1), which represent both the attractive oxygen and hydrogen sites. We have followed Ref.[13] and made the two attractive site of equal valence. This is also consistent with the MB symmetry of 2D water model, for which the oxygen and hydrogen sites are not distinguished and simply replaced by similar attractive sites, and the 3 arms should be identical. This seemingly unphysical equivalent of the real water is justified by the fact that such simple model is able to capture the physical properties of the associating liquids as well as some of the anomalies of real water, such as the maximum density, the minimum of compressibility and the two types of amorphous phases (dense HDL and expanded LDL).[13] In order to avoid misalignments of the 2 arms, it is necessary to introduce a single repulsive site (in magenta in Fig.1). The interactions have been taken similarly to our previous work for water, with a $1/r^{12}$ repulsion and a Yukawa form for hydrogen bonding part of the interaction between two atomic sites a and b:

$$v_{ab}(r) = 4\epsilon_{ab}\left(\frac{\sigma_{ab}}{r}\right)^{12} + 557\alpha_{ab}\frac{Z_a Z_b}{r}\exp\left[-\frac{(r-R_{ab})^2}{\kappa_{ab}}\right] \qquad (1)$$

where we use the Lorentz rule for the site diameters $\sigma_{ab} = (\sigma_a + \sigma_b)/2$ and the Berthelot rule for the energy parameters $\epsilon_{ab} = \sqrt{\epsilon_a \epsilon_b}$, where σ_a and ϵ_a are

the diameter and energy of site a, respectively. In what concerns the screened Coulomb Yukawa part Z_a is the valence of site a, and α_{ab} is the sign of the interaction between sites a and b. As can see, in Eq.(1), the second term is not really Coulomb like since $\alpha_{ab} \neq \alpha_a \alpha_b$. These coefficients are listed in the last row of Table 1. The coefficient 557 results from reducing the magnitude of the 3D Coulomb interaction, as was explained in Ref.[20] It is because of the large discrepancy of magnitude between the first and second term, that charged and uncharged atomic groups behave differently and produce the typical microstructure seen in associated liquids.

The alkyl tail atoms are modeled as neutral zero valence sites $Z_C = 0$. The position of these "carbon" atoms is decided using the following criteria. If one is to respect the shifted positions as in real alcohol models, as in the left column of Fig.1), then the 2D version model become chiral. This is illustrated by showing the two possible symmetrical configurations, which become distinct in 2D. To avoid this unnecessary features, we have modeled the alkyl tail as a linear sequence of carbon atoms. However, contrary to Ref.,[19] where the discs are tangent, we have chosen to merge them up to half diameter, except for the first carbon, which is placed at a higher distance, such that the hydroxyl head is more exposed, avoiding hindrance of Hbond. All outer atoms have been given the same diameter $\sigma_{i>3} = \sigma_1 = \sigma$, that of the hydroxyl head. Inner atoms of the hydroxyl head (blue and magenta sites) have the same diameter $\sigma_B = \sigma_{\text{blue}} = \sigma_2 = \sigma_M = \sigma_{\text{magenta}} = \sigma_3 = \sigma/3$.

The parameter of the alcohol models are summarized in the following Table 1 and Table 2.

σ	σ_B	σ_M	σ_C	ϵ	ϵ_B	ϵ_M	ϵ_C	Z_B	Z_M	Z_C	κ	R_i
1	1/3	1/3	1	1	1/2	1/2	1	0.3	0.15	0	0.15	0
$\alpha_{PP} = -1; \alpha_{PM} = 1; \alpha_{MM} = 1$; all other $\alpha_{ab} = 0$												

Table 1: Interaction parameters for 2D alcohols as in Eq.(1)

	O	B	M	C_1	C_n $(n = 2 - 8)$
r	0	1/3	1/3	3/4	$3/4 + (n-1)n$
θ	0	$\pm\pi/3$	0	π	π

Table 2: Site polar coordinates for 2D alcohols

2.2 Computational and theoretical details

Standard Monte Carlo simulation have been used in the constant N, V, T Canonical ensemble, a choice justified by the necessity to study structural properties with fixed number density $\rho_N = N/V$. The reduced density and temperature are defined in Lennard-Jones units related to the parameters of the polar head site O as $\rho = (N/V)\sigma^2$ and $T = k_B T_K/\epsilon$ (where T_K is the temperature in Kelvin). Three temperatures are studied, $T = 1$, $T = 2$ and $T = 3$, which

would correspond to liquid phases above the triple point. The densities vary between $\rho = 0.1$ and $\rho = 0.45$, the latter accessible only for methanol. A more appropriate density would the packing fraction $\eta = \rho S_n$, where S_n is the surface of the molecule which depends on the number of monomers n ($n = 1 - 8$)

$$S_n = (n+1)\frac{\pi}{4}\sigma^2 - 2L\left(\frac{\sigma}{8}\right) - 2nL\left(\frac{\sigma}{4}\right) \tag{2}$$

where $L(d)$ is the surface of the lens of a disc of diameter σ at distance d from the center.

$$L(d) = \frac{\sigma}{4}^2 \arccos\left(\frac{2d}{\sigma}\right) - \frac{d\sigma}{2}\sqrt{1 - \left(\frac{2d}{\sigma}\right)^2} \tag{3}$$

An alternative packing fraction $\eta^{(DR)} = \rho S_n^{(DR)}$ would be to scale according to the surface of the disco-rectangle $S_n^{(DR)}$ which contains the molecule

$$S_n^{(DR)} = \frac{\sigma^2}{4}(\pi + 1 + 2n) \tag{4}$$

The system sizes are taken to be large enough to ensure all site-site correlation to decay to the asymptote $g_{ab}(r) \to 1$ by $r = (1/3)L$ where L is the box size. This corresponds to $N = 700$ for methanol to $N = 336$ for octanol. The systems are started with square box configurations were all the particles are aligned. The number of particle is determined by the condition for a rectangle containing at most one particle to pave the entire box. Equilibration and production are about 50×10^3 steps, where one step consists in attempting to move all N particles successively. In the case of low temperature and longer alcohols, it is necessary to use 100 thousand steps. All pairs of site-site correlation functions $g_{ab}(r)$ between pairs of sites (a, b), as well as internal energies and virial pressures are evaluated during the production runs. The site-site structure factors are obtained by a 2D Fourier transform of the pair correlation functions:

$$S_{ab}(k) = 1 + \rho \int d\mathbf{r}\,[g_{ab}(r) - 1]\exp(i\mathbf{k}.\mathbf{r}) \tag{5}$$

The total structure factor is equally required

$$S_{ab}^{(T)}(k) = w_{ab}(k) + S_{ab}(k) - 1 \tag{6}$$

which involves the intra-molecular correlations, which for rigid molecules are defined as

$$w_{ab}(k) = j_0(kd_{ab}) \tag{7}$$

where d_{ab} is the distance between sites a and b inside the molecule. The 2D Fourier transforms are numerically evaluated by Talman transform techniques.[21,22] This step necessitate to convert the correlation functions $g_{ab}(r)$ from equal r-steps to log-scale. This is dont using a linear interpolation, which

adds small oscillatory artifacts visible in the k-range below $k\sigma \approx 0.05$. Finally, the scattering intensity is calculated with the equivalent of the Debye formula

$$I(k) = \alpha \sum_{a,b} f_a(k) S_{ab}^{(T)}(k) f_b(k) \tag{8}$$

where $f_a(k)$ is the form factor for atomic site a. Since there is no such thing as an atom form factor for 2D model atoms, we have used that of the normalized carbon atom form factor for all sites (see Fig.S1 in the SI document)

$$f_a(k) = f(k) = \frac{f_C(k)}{f_C(0)} \tag{9}$$

The coefficient α has a physical meaning in 3D, with $\alpha = r_0\rho$, where $r_0 = 2.8179 \cdot 10^{-13}$cm is the electronic radius. If we adopt the same convention in 3D, we can compare the 2D and 3D spectra, which is what we have done in the sub-Section3.4.

The various structure factors, intra-molecular correlations and form factor are illustrated in Fig.S1 of Supplemental Information (SI) document for the case of ethanol and octanol.

Thermodynamical properties such as the excess internal energy per particle E/N or the compressibility factor $Z = \beta P/\rho$ are illustrated for the case of ethanol and octanol in the SI document in Fig.S2.

3 Results

3.1 The microscopic structure

The microscopic structure of the alcohols can be see most directly by examining snapshots, which illustrates the clustering of the hydroxyl head groups into short chains of various topologies, mostly chains. Fig.2 illustrates for the case of ethanol the MB arm bonding scheme, which is at the base of the 2D hydrogen bonding model, and which is well captured by the site-site model.

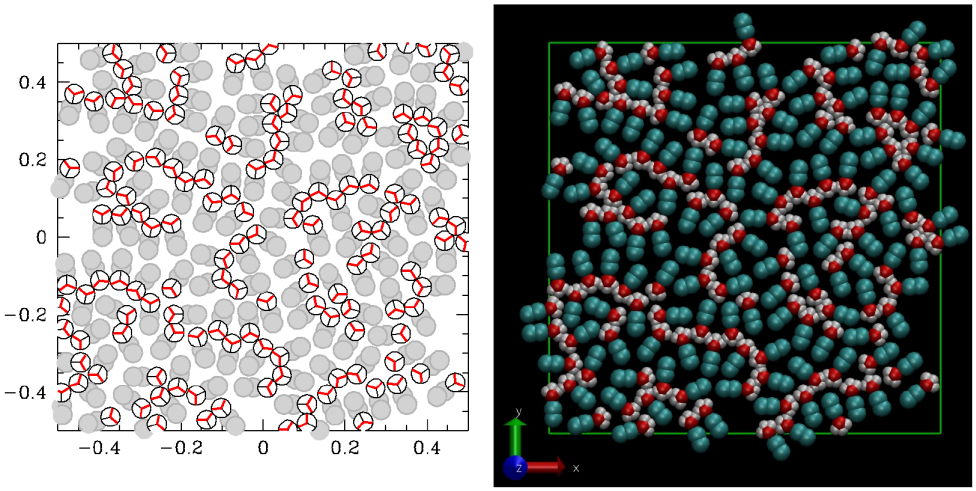

Figure 2: Snapshot for 2D ethanol illustrating the hydroxyl head clustering through MB arm alignments (left panel). This for for a $N = 144$ ethanol molecules system, for $T = 2$ and $\rho = 0.35$. The carbon atoms are shown in filled gray discs. The active MB arms are shown in thick red lines. The right panel is the VMD[23] rendering for comparison. The box border is shown in blue(expand to see).

While this is for a rather small system of $N = 144$ ethanol molecules, in practice, however, larger systems have been studied, which we examine now. The most important difference between the two snapshots is that the left panel shows more clearly that sites seemingly belonging to a large chain cluster, are not often sufficiently close enough to be considered as part of that cluster. In other words, although large chain clusters are apparent, a strict cluster analysis would show them as broken into smaller entities. This difference is not visible in the right panel, where only large chain cluster become apparent. We will consider only this type of snapshot below, since this is closer to what is seen in the spectral analysis (x-ray scattering for instance), as will be explained later.

Figs.3-5 show typical configuration for methanol, pentanol and octanol, thus covering the range from short($n = 1$), medium($n = 4$) and long($n = 8$) alcohols, where n is the number of methyl groups. Cases for typical high temperature ($T = 3$) and low temperature ($T = 1$) are shown for typical high and low densities.

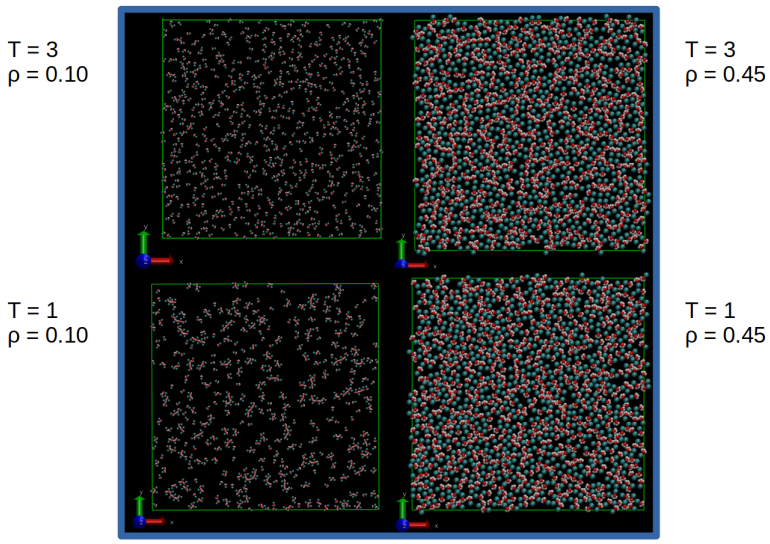

Figure 3: Snapshots for methanol for two different temperatures and densities. The plots are made using VMD.[23] Red disc for the hydroxyl head, with white sites representing the 3 inner bonding sites, and green sites for the alkyl tail C atoms. These systems concern $N = 700$ methanol molecules. The simulation box borders can be seen by expanding the figure.

What is clear, is that for all alcohol models, low density states look like a gas small clusters, whose size grows with decreasing temperature, while high density states are more clustered, with a similar temperature effect.

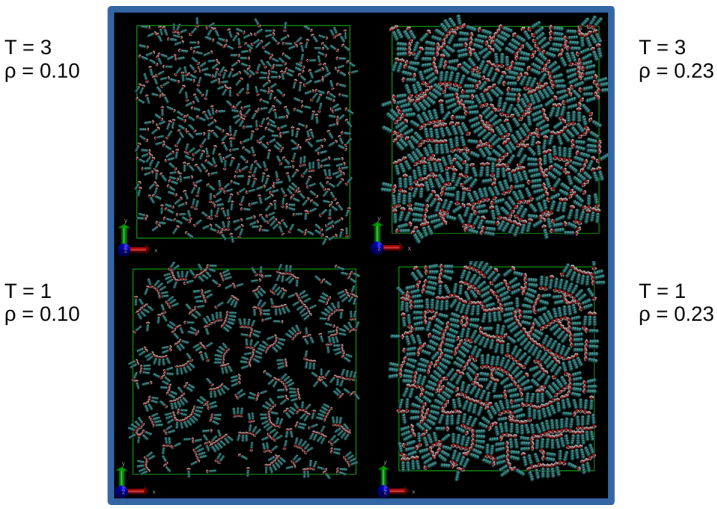

Figure 4: Snapshots for butanol for two different temperatures and densities. The plots details are as in Fig.3. The snapshots are shown for systems of $N = 468$ butanol molecules.

Interestingly, this trend is reversed for methanol dense liquid, where the high temperature state is seen to exhibit larger clusters. This is due to the smaller alkyl tail, which contributes less to the thermal induced disorder than when it is larger.

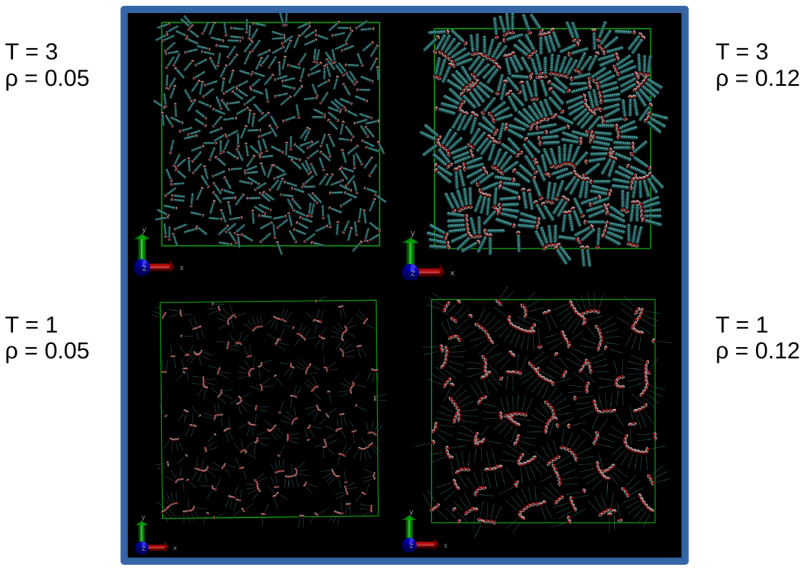

Figure 5: Snapshots for octanol for two different temperatures and densities. The plots details are as in Fig.3. The lower snapshots show the alkyl tails as sticks, such that the hydroxyl head clusters are more apparent. The snapshots are shown for systems of $N = 336$ octanol molecules.

For the case of octanol, only the polar heads are shown, which allows to see clearly the typical shapes of the clusters, ranging from chains, to y-shaped branched ones. Circular shapes occur more frequently for smaller alky tails.

3.2 Charge ordering through structural properties

The site-site correlation functions $g_{ab}(r)$ for a molecular liquid are defined as the statistical averaged second moment of the local density functions $\rho_a(\mathbf{r})$ and $\rho_b(\mathbf{r})$ for pairs of atoms (a, b) as if it was an atomic mixture of all the atoms in the molecule[7] :

$$g_{ab}(r) = \frac{1}{\rho_a \rho_b} < \rho_a(\mathbf{r}')\rho_b(\mathbf{r}") >$$

where $r = |\mathbf{r}' - \mathbf{r}"|$ and ρ_a is the number density of atomic species a. This definition may be complemented by the intra-molecular contribution $w_{ab}(r)$ corresponding to Eq.(7) if one wants to describe the molecular liquid. The important point is that the site-site function describes fluctuations of the local densities. In that, they will have particular features if some atomic clustering features occur. But this clustering is measured as a form of fluctuation. It is not a measure of clusters themselves. For instance, the molecule may be considered as a cluster of atoms, and it is measured by the $w_{ab}(r)$ intra-molecular part. But $g_{ab}(r)$ contains also information as how different atomic contacts occur outside the molecule.

The conventions for displaying correlation functions are illustrated in Fig.6 for the case of butanol for $T = 2$ and $\rho = 0.2$. In principle one should show the correlations and structure factors in normal scale (upper panels). However, because the strong dimerisation enhanced by the dimensional effect, the main peak of the $g_{ab}(r)$ are very narrow and high, much more than in the 3D case. Similarly, the pre-peak of the structure factors are as high, if not higher than the main peak, and the large k oscillatory structure is much more pronounced than in 3D. For these reasons, it appear convenient to use log scales for the abscissas (lower panels), which is the convention that we will adopt throughout.

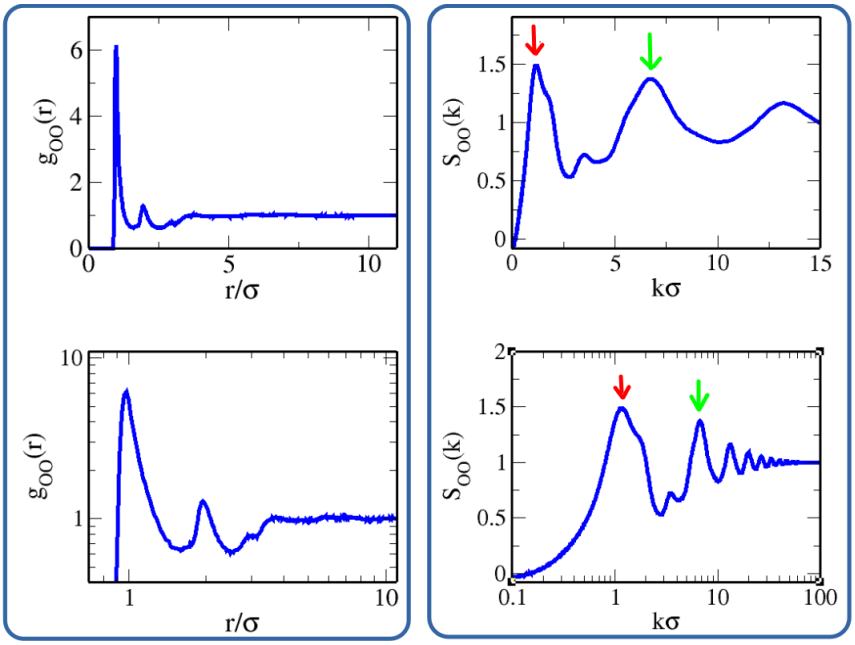

Figure 6: Conventions (see text) for structural functions illustrated for the case of butanol for $T = 2$ and $\rho = 0.2$. Left panel OO pair correlation function $g_{OO}(r)$: (top) normal scale, (bottom) log-log scale. Right panel, structure factor $S_{OO}(k)$: (top) normal scale, (bottom) semi log scale. The red and green arrows indicate the pre-peak and main peak positions, respectively. The bottom pictures conventions will be adopted throughout.

3.2.1 Oxygen-Oxygen correlations

Fig.7 shows the polar head ("oxygen" O atom) correlations at fixed packing fraction $\eta = 0.46475$ ($\eta^{(DR)} = 0.69$) for two different temperatures. The most remarkable feature, aside the high narrow first peak, is the extended depletion correlation that follows it, which is more marked with increasing alkyl tails. These depleted correlations witness the chain-like clustering (which depletes the O atoms from a spherical distribution around the central O atom). This is

more pronounced that in 3D because of the dimensional restrictions. In that, the 2D model allows to highlight spectacularly the main driving effects behind the clustering of alcohols. Lowering the temperature increases the first peak and extends both the depth and the width of the depletion correlations (lower panel).

c

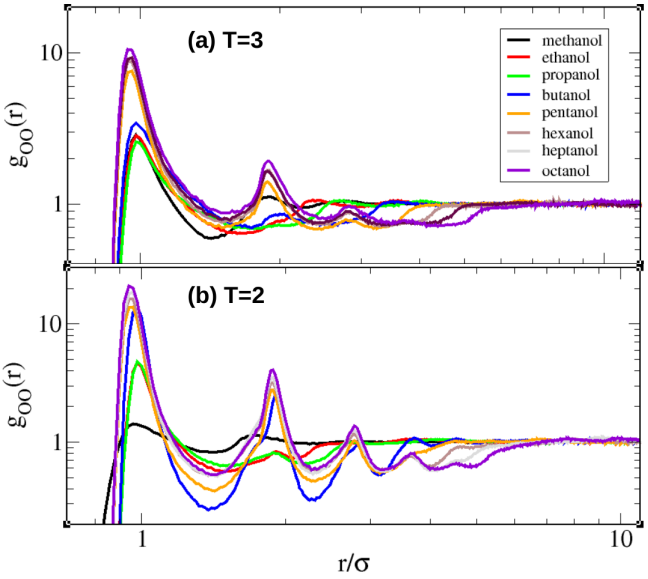

Figure 7: Oxygen-oxygen (polar head) correlation functions $g_{OO}(r)$ for all alcohols for 2 different temperatures $T = 3$ (upper panel) and $T = 2$ (lower panel) and for packing fraction $\eta \approx 0.465$. The color conventions are as in the legend in the upper panel.

The related structure factors Eq.(5) are shown in Fig.8. The most relevant feature is the prominent pre-peak, which is even much higher than the main peak, a feature never encountered in real alcohols.[16] This is of course a strict consequence of the depletion correlations in Fig.7.

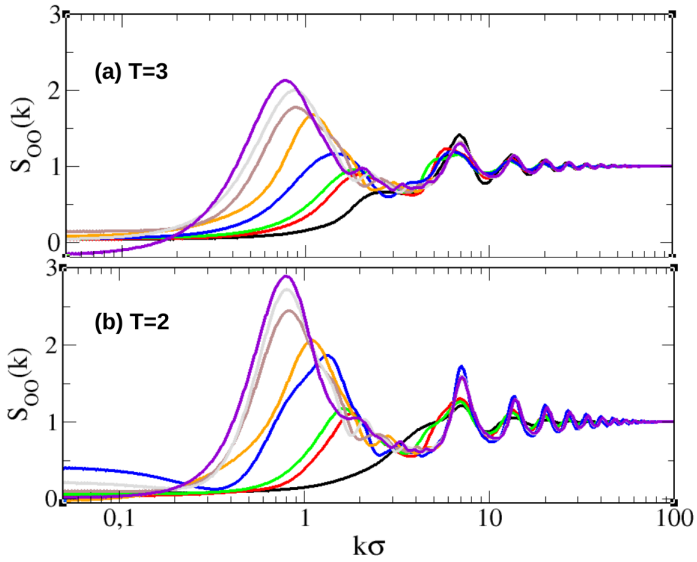

Figure 8: Oxygen-oxygen (polar head) structure factors $S_{OO}(k)$ for all alcohols for 2 different temperatures $T = 3$ (upper panel) and $T = 2$ (lower panel) and for packing fraction $\eta \approx 0.465$. The color conventions are as in the legend in Fig.7

The anomalous high temperature induced raise in clustering for methanol, described in the previous section, can be see here, as the black curve for T=3 has a more pronounced shoulder peak than for T=2 where the shoulder moves towards the main peak, hence signaling smaller clustering trends. Interestingly, the flat shoulder peak for methanol at T=3 is very similar to that in 3D,[16] which shows that the site model is pertinent enough to represent real 3D alcohols.

3.2.2 Influence of tail atoms

Fig.9 shows the correlation functions between the last carbon atoms for different alcohols. These curves show correlations that look very much Lennard-Jones like, hence are re presented with ordinary scale for the abscissa, unlike the previous ones. One can observe certain amount of depletion, specially for the longer alcohols (purple curve for instance), which makes sense in view of Figs4,5, which show the parallel stacking of the tails, hence a strong chain-like correlation between carbon atoms of same rank. Another interesting feature is the correlations for methanol (black curve) which show a higher first peak and lower second peak for T=3 and both peaks of similar height for T=2. This is a consequence of the high temperature clustering inversion discussed above, which is equally reflected in the carbon correlations.

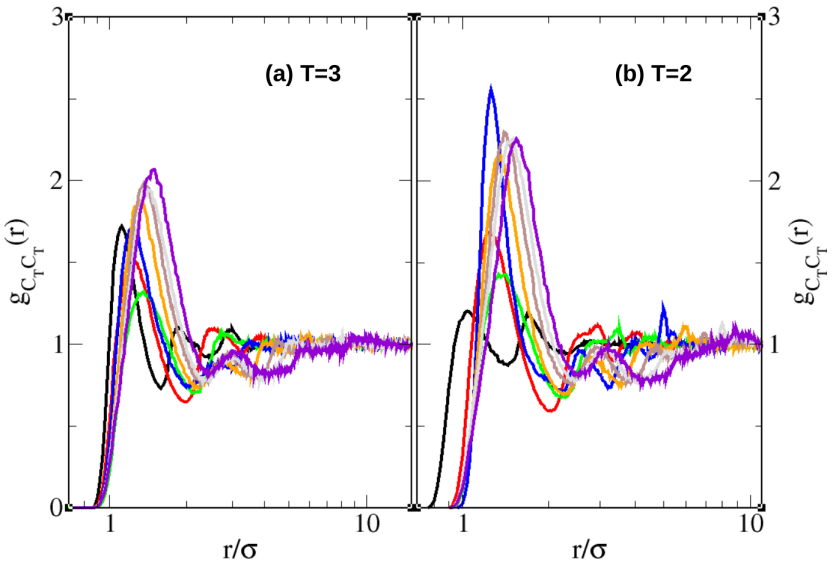

Figure 9: Last alkyl tail carbon-carbon pair correlation functions $g_{C_TC_T}(r)$ for all alcohols for 2 different temperatures $T = 3$ (upper panel) and $T = 2$ (lower panel) and for packing fraction $\eta \approx 0.465$. The color conventions are as in the legend in Fig.7

Fig.10 shows the corresponding structure factors. Interestingly, these structure factor show prominent pre-peak, which are also seen in 3D alcohols, but mostly for longer ones. In the 2D case, all alcohols show a pre-peak, which is nevertheless not of the same magnitude as that of the O-O correlations, since these at most equal the main peak height for most alcohols. Indeed, these correlations are a consequence of the O-O Hbonding, and the depletion correlations are not as important, as was observed in Fig.9. We note that the methanol structure at T=3 has again this interesting charge order inversion with respect to T=2.

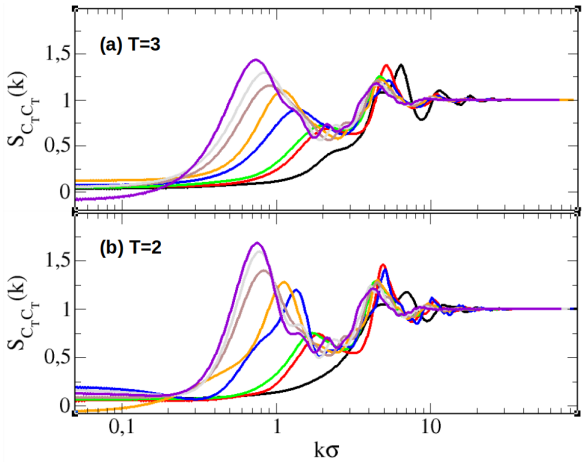

Figure 10: Last alkyl tail carbon-carbon structure factors $S_{C_TC_T}(k)$ for all alcohols for 2 different temperatures $T = 3$ (upper panel) and $T = 2$ (lower panel) and for packing fraction $\eta \approx 0.465$. The color conventions are as in the legend in Fig.7

The depletion correlations, observed for all atom correlations, although illustrated only in particular cases above, are a direct consequence of the charge order correlations, where O-P-O chain-like ordering is observed, similar the hydrogen bond correlations O-H-O in real alcohols. In the next section we illustrate how such correlations result from charge ordering.

3.2.3 Charge-charge correlations

Fig.11 shows the pair correlation functions between the "charged" sites. The most interesting feature is the fact that the cross charge correlations are intermediate between the blue and magenta correlations, as witnessed by the first neighbour peaks. This cascade results exactly from the charge order, as blue sites tend to stick together, and the magenta sites are the most repelled. This is a 2D mimicry of the 3D situation where positive and negative charges attract each other, contributing to a high peak[24] , while the like charge correlations are moved to large distances: the green curve is out of phase with respect to the blue and magenta curves which are more or less in-phase.

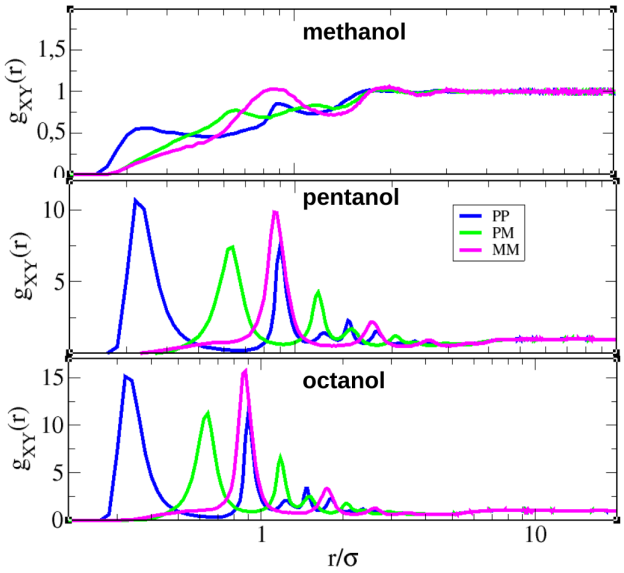

Figure 11: Charged sites pair correlations between the blue and magenta sites, for three typical alcohols from the smallest (upper panel, methanol: $n = 1$) to the longest (lower panel, octanol: $n = 8$), with the intermediate pentanol (middle panel: $n = 5$). All curves are for packing fraction $\eta \approx 0.465$ and $T = 2$.

Fig.12 shows the resulting structure factors. Interestingly, although the pair correlations look very dissimilar, their contributions to the pre-peak are almost identical. The differences are seen in the main peak positions, which reflect directly those of the corresponding $g_{XY}(r)$. In particular, in the case of the pentanol and octanol, it is clearly seen that the cross charge correlations green curve is an anti-peak to the main peak of the blue and magenta of the like charge correlations. This is very similar to that observed in the case of the 3D ionic liquids[25] , and is the symptom of the charge ordering process.

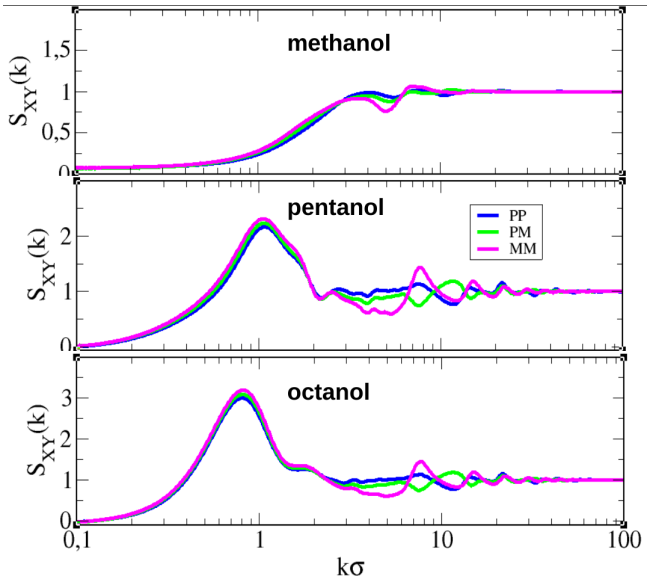

Figure 12: Charged sites structure factors between the blue and magenta sites, for three typical alcohols from the smallest (upper panel, methanol: $n = 1$) to the longest (lower panel, octanol: $n = 8$), with the intermediate pentanol (middle panel: $n = 5$), and corresponding to the pair correlation functions in Fig.11.

We will return to charge ordering when examining the scattering intensities in Section 3.4.

3.3 Clustering

Instead of the pair correlations which represent cluster fluctuation, computer simulations allow to probe the clusters themselves, as for instance the clusters of the O-atoms, by building the histogram of groups of atoms pairs separated by typically the distance which corresponds to the first minimum of $g_{OO}(r)$.[16] The corresponding normalized cluster probabilities $P(s)$ versus cluster size s are shown in Fig.13 for 3 different alcohols, methanol, pentanol and octanol, and for 3 temperatures and various densities. The first striking feature is that all these curves is that they very much exponential-like, without however the typical cluster peak at s$= 5 - 7$ observed in neat alcohols[16] .

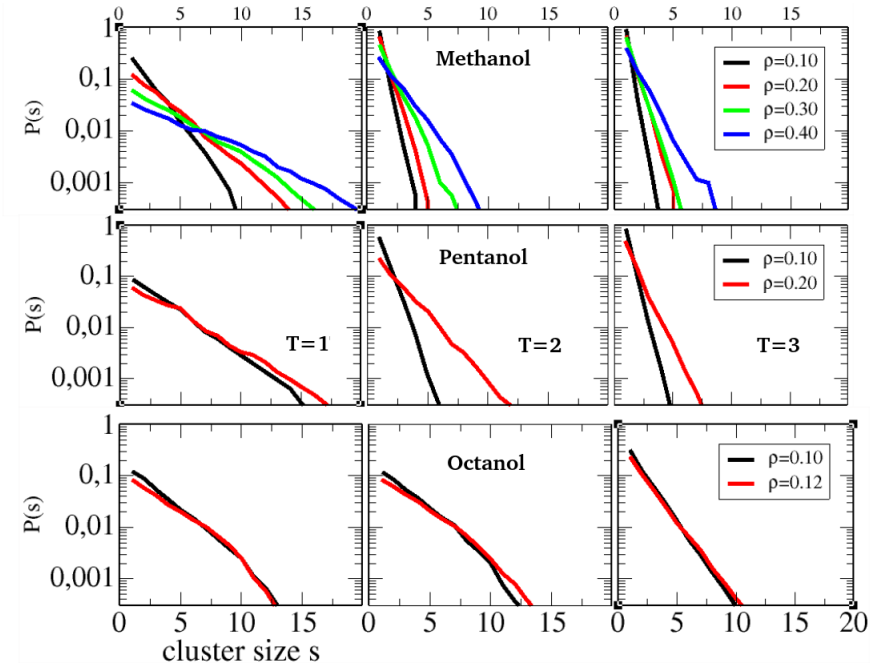

Figure 13: Normalized cluster distribution $P(s)$ for methanol (upper 3 panels), pentanol (middle 3 panels) and octanol (lower 3 panels), for three different temperatures (a) all left panels T=1, (b) all middle panels T=2 and (c) all right panels T=3. For each temperature, the evaluated densities are shown on the inset of the left panels.

The absence of the cluster peak, when the snapshots show clear charged group chain aggregate is intriguing. In fact, as mentioned in Section 3.1, a closer look at the chain clusters show that most of them are broken into smaller aggregates, and this is what a strict cluster analysis shows. This means that, even though clear chain-like "domain" of the hydroxyl head group can be observed in simulations, these represent in fact fluctuating domains containing strict clusters. What the pair correlation functions measure are these fluctuating "domains", just like the visual analysis would suggest. I am tempted to suggest that it is these labile domains which represent the true clusters in term of micro-structure. In real 3D alcohols, the strict clusters are stabilized by dimensional effects, such as the fact that the alkyl tails surround the polar head chain clusters and "block" their fluctuations, and this produced the typical cluster peak.

A closer analysis shows trends of $P(s)$ which can be expected, such as $P(s)$ becomes more exponential at high T because of increasing disorder, or $P(s)$ for low density decays faster than for high density, because clusters are larger at high density. These trends are less marked for larger alcohols, which is equally expected, from the observation of the snapshots.

3.4 Scattering properties

Eq.(8) allows to calculate the equivalent of x-ray scattering in real units from the total structure factors calculated for the model alcohols studied herein. Such x-ray intensities are shown in Fig.14 for methanol and Fig.15 for propanol and both are compared with the respective calculated spectra for the OPLS model of the real alcohols in ambient conditions,[16] shown as gray curve. The k values are arbitrarily scaled with $\sigma = 3.5\mathring{A}$, which is approximately the diameter of the carbon atom in 3D force field models. This comparison illustrates both the pertinence of the present 2D models and the differences between real alcohol clustering and the model, from the perspective of radiation scattering.

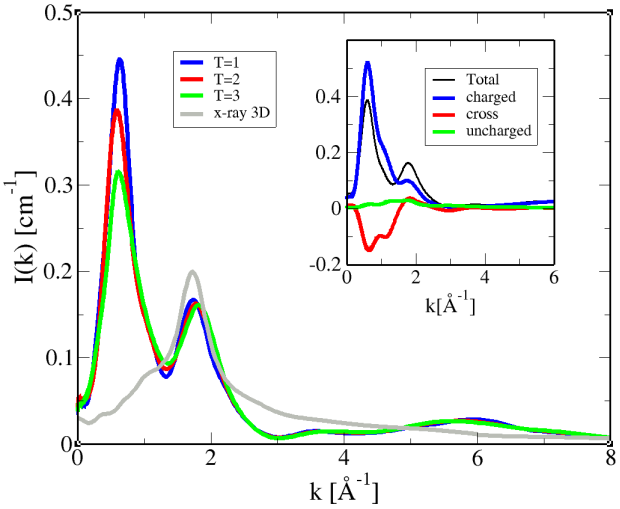

Figure 14: Calculated x-ray scattering intensities for the 2D methanol model for $\rho = 0.45$ and 3 different temperatures $T = 1, 2, 3$, and compared with that from the OPLS model of real ambient condition methanol (gray curve) from Ref.[16] The inset shows the partial contributions to $I(k)$ (black curve) for $T = 2$, from charged atomic groups (blue), uncharged ones (green), as well as the cross contributions (red).

The calculated 2D spectra are displayed for 3 different temperatures, and the amplitudes are seen to increase with decreasing temperatures, a trend similar to that observed for real alcohols.[16] The similarities of the main peak contributions at $k \approx 1.5\mathring{A}^{-1}$ for both alcohols and their realistic counter part is striking, both in terms of amplitude and position. In fact, this is not unlike the comparison of the Lennard-Jones liquid structure factors for 2D and 3D which are equally very much comparable. In other words, it is simply the expression of packing effect in any dense liquid. The pre-peaks, however, are a different matter. For both alcohols, the pre-peak positions are shifted to smaller-k values, indicating that the 2D clusters are larger than their 3D counter parts. The amplitudes are also

much higher, specially for methanol. If we interpret the amplitude as related to the density of the cluster, then it make sense since there are more clustering in 2D than in 3D. This is again particularly true for methanol, as seen in Fig.3.

c

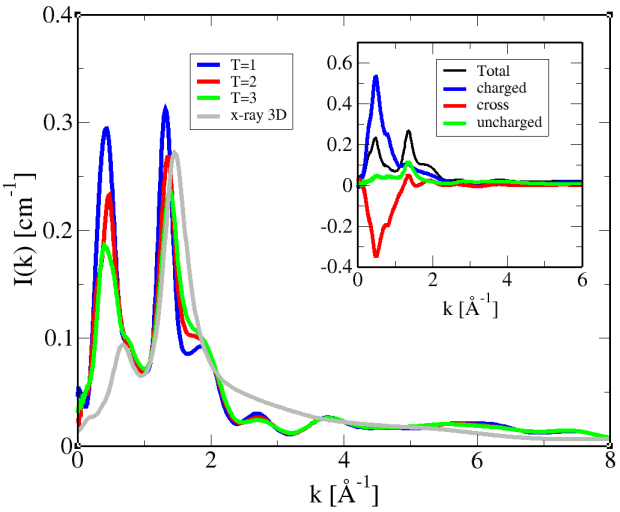

Figure 15: Calculated x-ray scattering intensities for the 2D propanol model for $\rho = 0.30$ and 3 different temperatures $T = 1, 2, 3$, and compared with that from the OPLS model of real ambient condition propanol (gray curve) from Ref.[16] The inset shows the partial contributions to $I(k)$ (black curve) for $T = 2$, from charged atomic groups (blue), uncharged ones (green), as well as the cross contributions (red).

When the interpretation of the pre-peak position in term of labile cluster "size" is justified, this is not the case for the amplitudes. Indeed, the insets of both figures show the charged (polar), uncharged (apolar) and cross contributions to the total spectra

$$I(k) = I_{\text{charged-charged}}(k) + I_{\text{uncharged-charged}}(k) + I_{\text{cross}}(k) \qquad (10)$$

where each term consists in selecting the appropriate atoms in the sum in the Debye formula Eq.(8), illustrated for for $T = 2$. While it is seen that all 3 contributions are positioned around $k_P \approx 0.5\mathring{A}^{-1}$, suggesting a mean cluster size of $R_c = 2\pi/k_P \approx 12\mathring{A}$, the positive and negative contributions to the amplitude do not allow to decide if the resulting amplitude concerns the density of the clusters.

The separation of $I(k)$ in three different contributions has been discussed in the case of the 3D liquids[16] . The positive pre-peak of the charge-charge contribution is essentially due to the 2 factors[24] , the very high and narrow first neighbour correlations and the depletion of the second and higher neighbour

(as in Fig.7). The negative pre-peak, or anti-peak, is the mostly result of the correlations between the charged and the uncharged groups being depleted from the first neighbours, for obvious reasons since these 2 types of atoms do not interact through the pseudo-Coulomb term in Eq.(1).

The intra-molecular terms contribute importantly to the magnitude of the pre and anti peaks, as illustrated by Fig.S1 in the SI document.

4 Discussion and conclusion

Perhaps the most interesting feature presented in this work is the fact that a mimicry of the real Coulomb interaction as in the second term of Eq.(1) is sufficient to produce charge ordering and correlations effects very similar to that observed in real molecular liquids and alcohols. Indeed, equation (1) contains two terms of vastly different magnitudes, specially when the valences Z_i of atomic sites i are non-zero. This pseudo-Coulomb model works very well for modeling 2D ionic liquids,[20,26] even with neutral groups attached to charged ones (the so-called room temperature ionic liquids in the realistic 3D case[27]). The model would allow to mix such ionic species with the present polar species, and study in two-dimension various interesting phenomena observed for realistic mixtures. Since the pair interactions between the charged groups are taken into account, the study of electrolytes and aqueous mixtures becomes possible, and do not require any extra hypothesis as in the case of the MB model and variants[28,29] .

The present work is focused on the micro-structure of 2D associated liquids, as seen from the site pair correlation functions and corresponding structure factors. It helps better define the concept of cluster, as a necessarily fluctuating entity, for which fluctuations play an essential role in structuring the system. The concept of mean cluster as referring to tightly bound atomic sites, does not allow to explain the features observed in the radiation scattering intensity, as was demonstrated herein. This concept refers to a "particle" instead of referring to a "fluctuation". Yet, both representations are conceivable and the first has been abundantly used in the literature. I have previously suggested to use the better adapted concept of the duality between aggregation and fluctuation.[6] The present work serve to illustrate how this concept is embodied in the behaviour of the density pair correlation functions and their transforms, including a toy presentation of x-ray scattering in 2D liquids. I expect to extend this study to model self-assembly, such as that present in soft matter, where the scattering pre-peak is often used to describe the self-assembled "objects" from strict cluster point of view. The fluctuation point of view may bring interesting surprises.

References

[1] Ising, E. Beitrag zur theorie des ferromagnetismus. *Zeitschrift für Physik* **1925**. *31*, 253–258.

[2] Landau, L.; Lifshitz, E. *Statistical Physics: Volume 5*. vol. 5. Elsevier Science, **2013**.

[3] Chaikin, P.; Lubensky, T. *Principles of Condensed Matter Physics*. Cambridge University Press, **2000**.

[4] Alder, B. J.; Wainwright, T. E. Phase transition in elastic disks. *Physical Review* **1962**. *127*, 359–361.

[5] Saija, F.; Prestipino, S.; Giaquinta, P. V. Entropy, correlations, and ordering in two dimensions. *The Journal of Chemical Physics* **2000**. *113*, 2806–2813.

[6] Perera, A. From solutions to molecular emulsions. *Pure and Applied Chemistry* **2016**. *88*, 189–206.

[7] Hansen, J.; McDonald, I. *Theory of Simple Liquids*. Elsevier Science, **2006**.

[8] Dupuy, J.; Dianoux, A. J., (Eds.) *Microscopic Structure and Dynamics of Liquids*. Springer New York, NY, **1978**.

[9] Eaves, J. D.; Loparo, J. J.; Fecko, C. J.; Roberts, S. T.; Tokmakoff, A.; Geissler, P. L. Hydrogen bonds in liquid water are broken only fleetingly. *Proceedings of the National Academy of Sciences* **2005**. *102*, 13019–13022.

[10] Finney, J. L. The structure of water: A historical perspective. *The Journal of Chemical Physics* **2024**. *160*, 060901.

[11] Ben Naim, A. Statistical Mechanics of Waterlike Particles in Two Dimensions. I. Physical Model and Application of the Percus - Yevick Equation. *The Journal of Chemical Physics* **1971**. *54*, 3682–3695.

[12] Brini, E.; Fennell, C. J.; Serra, M. F.; HribarLee, B.; Lukšić, M.; Dill, K. A. How waterâs properties are encoded in its molecular structure and energies. *Chemical Reviews* **2017**. *117*, 12385–12414. PMID: 28949513.

[13] Baré, T.; Besserve, M.; Urbic, T.; Perera, A. A site-site interaction two-dimensional model with water like structural properties. *Journal of Molecular Liquids* **2023**. *386*, 122475.

[14] Amann-Winkel, K.; Bellissent-Funel, M.-C.; Bove, L. E.; Loerting, T.; Nilsson, A.; Paciaroni, A.; Schlesinger, D.; Skinner, L. X-ray and neutron scattering of water. *Chemical Reviews* **2016**. *116*, 7570–7589.

[15] Perera, A. On the microscopic structure of liquid water. *Molecular Physics* **2011**. *109*, 2433–2441.

[16] Požar, M.; Bolle, J.; Sternemann, C.; Perera, A. On the x-ray scattering pre-peak of linear mono-ols and the related microstructure from computer simulations. *The Journal of Physical Chemistry B* **2020**. *124*, 8358–8371.

[17] Hura, G.; Russo, D.; Glaeser, R. M.; Head-Gordon, T.; Krack, M.; Parrinello, M. Water structure as a function of temperature from x-ray scattering experiments and ab initio molecular dynamics. *Phys. Chem. Chem. Phys.* **2003**. *5*, 1981–1991.

[18] Barbara, H.; A., D. K. Modeling simple alcohols in two dimensions. *Acta chimica slovenica* **2006**. *53*, 257 – 263.

[19] Papez, P.; Urbic, T. Simple two-dimensional models of alcohols. *Phys. Rev. E* **2022**. *105*, 054608.

[20] Perera, A.; Urbic, T. Charge ordering in two-dimensional ionic liquids. *Physica A: Statistical Mechanics and its Applications* **2018**. *495*, 393–404.

[21] Talman, J. D. Numerical fourier and bessel transforms in logarithmic variables. *Journal of Computational Physics* **1978**. *29*, 35–48.

[22] Ferreira, P. G.; Perera, A.; Moreau, M.; Telo da Gama, M. M. The hard ellipse liquid: An integral equation study. *The Journal of Chemical Physics* **1991**. *95*, 7591–7602.

[23] Humphrey, W.; Dalke, A.; Schulten, K. VMD – Visual Molecular Dynamics. *Journal of Molecular Graphics* **1996**. *14*, 33–38.

[24] Perera, A. Charge ordering and scattering pre-peaks in ionic liquids and alcohols. *Phys. Chem. Chem. Phys.* **2017**. *19*, 1062–1073.

[25] Perera, A.; Mazighi, R. Simple and complex forms of disorder in ionic liquids. *Journal of Molecular Liquids* **2015**. *210*, 243–251. Mesoscopic structure and dynamics in ionic liquids.

[26] Perera, A.; Urbic, T. Clustering in complex ionic liquids in two dimensions. *Journal of Molecular Liquids* **2018**. *265*, 307–315.

[27] Hettige, J. J.; Araque, J. C.; Margulis, C. J. Bicontinuity and multiple length scale ordering in triphilic hydrogen-bonding ionic liquids. *The Journal of Physical Chemistry B* **2014**. *118*, 12706–12716. PMID: 25157443.

[28] Aupic, J.; Urbic, T. Thermodynamics and structure of a two-dimensional electrolyte by integral equation theory. *The Journal of Chemical Physics* **2014**. *140*, 184509.

[29] Hribar, B.; Southall, N. T.; Vlachy, V.; Dill, K. A. How ions affect the structure of water. *Journal of the American Chemical Society* **2002**. *124*, 12302–12311. PMID: 12371874.